A Modular Dielectric Elastomer Actuator to Drive Miniature Autonomous Underwater Vehicles

Florian Berlinger*, Mihai Duduta*, Hudson Gloria, David Clarke, Radhika Nagpal, and Robert Wood

***Abstract*— In this paper we present the design of a fin-like dielectric elastomer actuator (DEA) that drives a miniature autonomous underwater vehicle (AUV). The fin-like actuator is modular and independent of the body of the AUV. All electronics required to run the actuator are inside the 100 mm long 3D-printed body, allowing for autonomous mobility of the AUV. The DEA is easy to manufacture, requires no pre-stretch of the elastomers, and is completely sealed for underwater operation. The output thrust force can be tuned by stacking multiple actuation layers and modifying the Young's modulus of the elastomers. The AUV is reconfigurable by a shift of its center of mass, such that both planar and vertical swimming can be demonstrated on a single vehicle. For the DEA we measured thrust force and swimming speed for various actuator designs ran at frequencies from 1 Hz to 5 Hz. For the AUV we demonstrated autonomous planar swimming and closed-loop vertical diving. The actuators capable of outputting the highest thrust forces can power the AUV to swim at speeds of up to 0.55 body lengths per second. The speed falls in the upper range of untethered swimming robots powered by soft actuators. Our tunable DEAs also demonstrate the potential to mimic the undulatory motions of fish fins.**

I. Introduction

Soft actuators are desirable for tasks such as locomotion because they are generally safer and more adaptable to unstructured environments than their rigid counterparts [1]. Soft actuators constitute an important step forward towards entirely soft robots [2], [3], and towards potential applications such as wearable and medical devices [4]. The most demanding component of any soft robot is the actuator used to propel it. While pneumatic and hydraulic actuators dominate the field, they are generally more suitable to tethered applications, such as grippers [5], [6], due to the equipment needed to provide pressure for actuation. However, as soft robotic applications shift towards autonomous operation and aim to match the properties of living systems [7], more options for soft, powerful, and scalable actuators are needed.

When actuators are small, easy to manufacture and require small power supplies, they become suitable for cooperative robotics and swarms of untethered robots [8]. Electroactive polymers (EAPs) are an attractive solution for mesoscale actuation because they directly convert electrical energy from a high energy density battery into a mechanical output [9]. Of the existing EAP technologies, dielectric elastomer actuators (DEAs) appear most suitable to function as soft actuators propelling a robot because of their large strain and high energy density [10] as well as fast response capability [11]. One of the central limitations of DEAs is the need for high actuation voltages—on the order of 1-10 kV—which often require large and heavy power supplies. By focusing on a swimming robot, the weight of the power supply is balanced by buoyancy, while the volume can be reduced by employing high performance power converters. Another limitation is the need for pre-stretch, which in most cases merges the actuator with the robot body and thereby constrains design

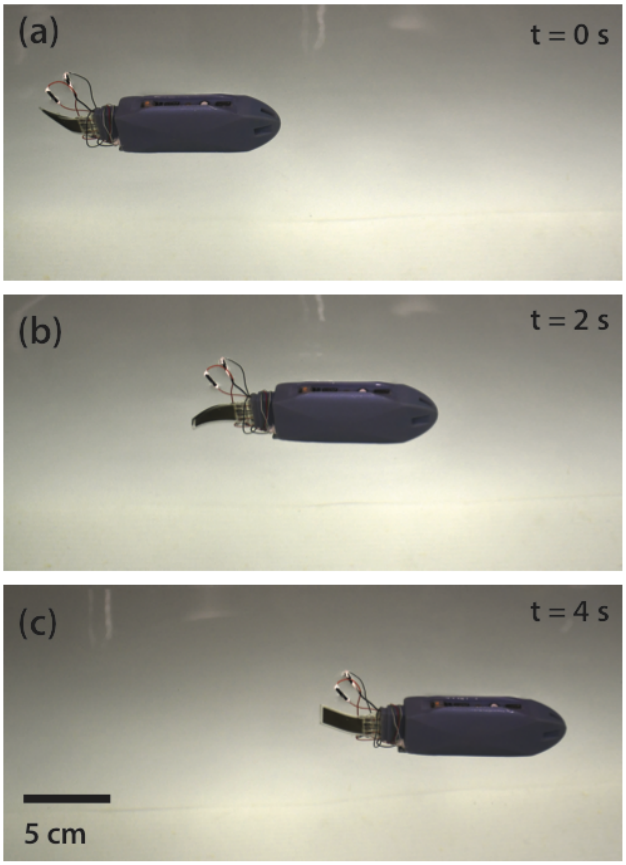

Fig. 1. Untethered DEA-powered robot during an open-loop swimming experiment in three separate instances, showing a top speed of 0.55 body lengths per second or 55 mm/s respectively.

*These authors contributed equally to the work. The research was supported by the National Science Foundation (Materials Research and Engineering Center - MRSEC - grant number DMR14-20570), the Wyss Institute for Biologically Inspired Engineering, and the Link Foundation. Any opinions, findings, and conclusions or recommendations expressed in this material are those of the authors and do not necessarily reflect the views of the National Science Foundation.

The authors are with the John A. Paulson School of Engineering and Applied Science at Harvard University, Cambridge, Massachusetts. Florian Berlinger, Mihai Duduta, Robert Wood, and Radhika Nagpal are also with the Wyss Institute for Biologically Inspired Engineering, Boston, Massachusetts. E-mails: {fberlinger@seas, mduduta@g, clarke@seas, rjwood@eecs, rad@eecs}.harvard.edu

choices. Additionally, pre-stretch adds considerable stiffness to the actuator and limits how much it can deform. By modifying the chemistry of the elastomer, we avoid the need for pre-stretch [12] which opens the possibility of using DEAs as soft and bio-mimetic actuators. Given the need for better soft actuators at the mesoscale, our goal was to build an untethered DEA-powered swimming robot to serve as a stepping stone in two directions: towards fully soft swimming robots and towards cooperative swarms of mesoscale robots.

To this end, we built a modular multilayer DEA capable of powering a miniature underwater vehicle (Figure 1). Our contribution is the integration of a soft and powerful actuator into a small and fully self-contained package that can be easily mounted on AUVs of various shapes. The fabrication of the actuator is straightforward as no pre-stretch of the elastomer is required. The sealing requirements are minimal as only four wires per actuator penetrate the vehicle's body. Several actuation layers can be stacked to increase the total actuator power output. Design guidelines for the development of powerful fin-like DEAs are detailed in Section III. The reconfigurable and miniature AUV is shown in Section IV. Results including measurements of thrust and speed as well as planar swimming and vertical diving are discussed in Section VI.

II. Related Work

At the most basic level, dielectric elastomers are compliant capacitors in which the applied electric field causes attraction between the electrodes (Figure 2(a)). Several strategies have been employed to convert that biaxial expansion into more useful bending motions, usually by incorporating constraining fibers or frames [13], [14]. The usage of DEAs in autonomous and mobile robots is novel albeit their development goes back to the 1990s. One major limitation of DEA-powered robots is the need for pre-stretch in the elastomer, which severely limits the types of motions available and makes the robot very specialized in how it can move. Across the board, including our earlier work [11], almost all DEA-powered robots use most of the robot body for small displacement deformations which propel the robot forward.

Early robotic applications were almost all tethered because of the need for large actuation voltages and the resulting size and mass of the power supply [15]. The first robot capable of carrying its own power supply [16] demonstrated untethered walking at a slow pace (0.001 BL/s)[1]. More recently, Jordi et al. [17] demonstrated a remote-controlled airship driven by DEAs. The actuators alternately contract the sides of the fish-like robot to generate forward propulsion. Offsetting the heavy electronics with lighter gas-filled sections resulted in a volume as large as an automobile.

For swimming robots, the only untethered example is an electronic fish by Li et al. [18], which reaches speeds of up to 6.4 cm/s (= 0.69 BL/s). The robot uses a pre-stretched membrane at the center of the body to power passive fins in a sting ray inspired configuration. Their 93 mm long robot uses the surrounding medium (water) as ground in order to facilitate the insulation of the high voltage actuators. The robot is therefore coupled with its environment; several such robots in a single tank of water might cause unsafe voltages. Shintake et al. [19] presented tethered biomimetic underwater robots, which are capable of either vertical or horizontal motion, depending on how the robot is built. The DEA in the fish-like design is spread over a thin and bendable 120 mm long body. Their fish-like robot achieved top speeds of 8 mm/s (= 0.07 BL/s). Other work includes a jellyfish inspired dive-capable robot [20] which also makes use of a pre-stretched dielectric elastomer membrane.

Dielectric elastomer actuators have unique advantages in an untethered swimming demonstration compared to other soft actuation technologies. Since DEAs are electrically powered, their power supplies could be smaller and with fewer components than those used by fluidic elastomer actuators [7] generally viewed as fast swimmers (0.4-0.95 BL/s). Other electrically powered actuators, such as ionic polymer-metal composites (IPMCs) are generally slower [21] (0.1 BL/s), [22] (0.05 BL/s) due to limitations of ionic diffusion compared to fast switching of electric fields. Lastly, shape memory alloys (SMAs) can be driven to swim fast by relatively compact power electronics [23] (0.2 BL/s), [24] (0.95 BL/s), but require more complex fabrication and integration of rigid and soft components. With our approach, DEA-powered swimming robots could be made as fast as fluidic or SMA-powered robots, while maintaining a small footprint of the power electronics and a simple fabrication process of the actuator.

Our multilayered actuator differs from the existing body of work on DEAs because: (i) our actuator is modular and independent of the robot body as opposed to [17], [18], [19], [20]; (ii) the low footprint power supply makes our robot autonomous compared to [19], [20]; (iii) the elastomer, size, shape, and final deformed shape of the actuator can each be independently tuned to match a desired target of thrust, speed, etc. Beyond these major advances, our actuator is sealed and safe to operate in water which allows for collective operation of multiple DEA-powered robots. Moreover, the fins are active, meaning the soft material deforms to propel the robot in a similar fashion to how biological systems swim. Such soft and tunable actuators could be used for robotics-inspired biological studies to better understand underwater locomotion. We present the design and working principle of our DEA in the following section.

III. Actuator Design

In our earlier work we described a reliable method to build multilayer DEAs that can be made into fast unimorph bending actuators [11], [12]. Following the same reasoning as other research groups [25], we adapted the method to produce bimorph actuators which can flap and propel a swimming robot. Two similar unimorph actuators are bonded

[1]The normalized metrics of body lengths (BL) and body lengths per second (BL/s) allow a fair comparison among similarly-sized robots.

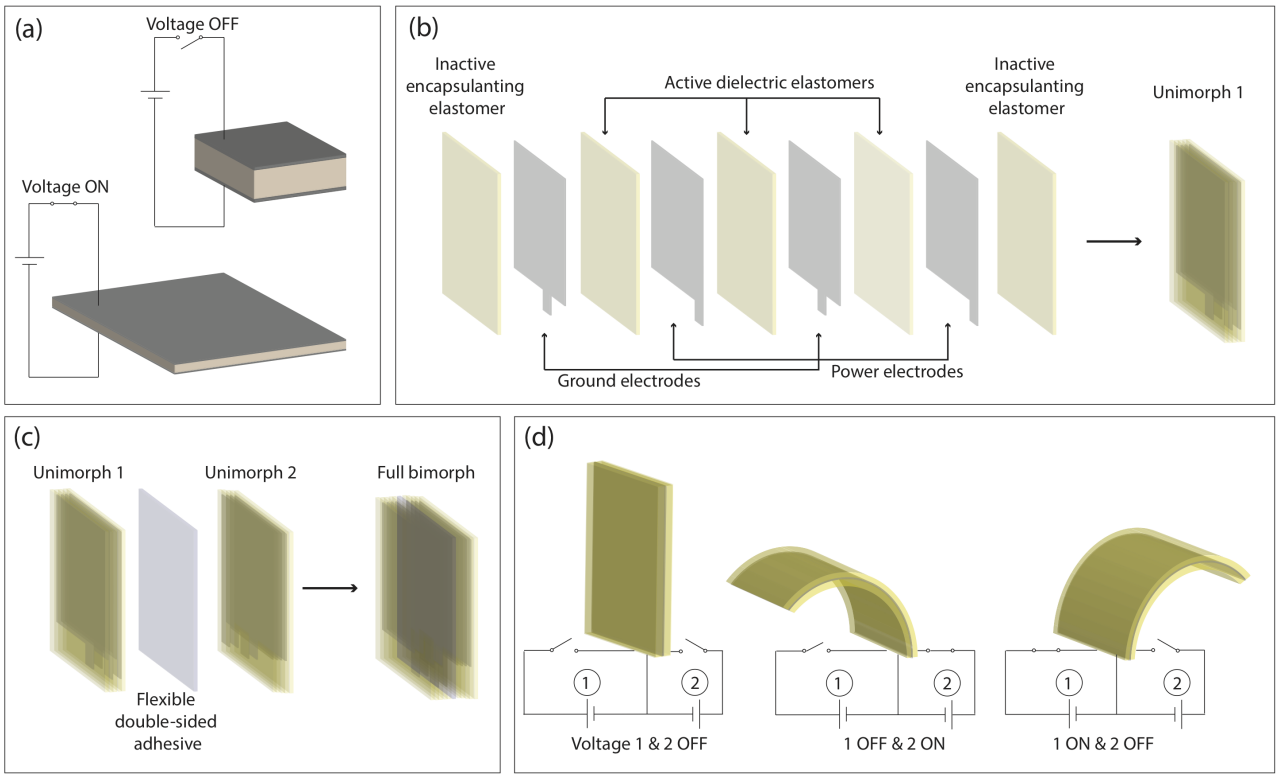

Fig. 2. (a) Working principle of a dielectric elastomer: biaxial expansion without constraints. (b) Assembly of a unimorph from three active dielectric layers, four electrodes and two encapsulating layers. (c) Formation of a bimorph from two unimorphs and a flexible adhesive. (d) Operation of a bimorph actuator. The two multilayer actuators comprising the bimorph are shown in a simplified way as elastomers attached by a flexible adhesive. The bottom of the stack is taken to be the mechanical ground, which for instance can be rigidly attached to a robot.

by a flexible double-sided adhesive (82600 from 3M Corporation, St. Paul, MN) to create a bimorph architecture as shown in Figure 1(c). When one half of the bimorph is actuated, the second half and the adhesive serve as a non-stretchable constraint, directing the actuator to bend, as shown in Figure 1(d). We used a model developed earlier [11] to guide the selection of layer thickness, number of layers as well as the applied voltage. When testing full bimorphs in water we discovered the model predictions to be optimistic higher bounds due to localized electrical breakdown in the elastomer. However, we considered the low fabrication yield versus high thrust trade-off to be valuable. We report on the bimorphs which had a low concentration of defects in the electrodes and produced the highest thrust as existence proof of the technology.

The applied voltage was fixed to 2 kV to minimize the chance of electrical breakdown. Since the actuator thrust output dictates swimming performance, we modified the design parameters, such as stiffness and number of layers, to increase the thrust output. The setup and method of measuring thrust is described in detail in Section V. The actuator active area was limited to 20 mm $\times$ 25 mm by the size of the single-walled carbon nanotube (SWCNT) transfer filter. The results of the impact study for number of layers, material stiffness, and the relative trade-offs are discussed in Section VI. For consistency and to link with the spin coating steps during fabrication, the bimorphs are labeled with the total number of layers (including sealing layers) per each unimorph. For example, a 17 layer fin includes two 17 layer unimorphs held together by a layer of double sided adhesive. The unimorphs can be made in parallel on a large wafer meaning that the total process time is dictated by the number of spin coating steps.

Each multilayer was built with an inactive base and top soft elastomer layer (0 % crosslinker corresponding to a Young's modulus of 50 kPa) which provided insulation from the water environment. The elastomer formulation was based on acrylic urethane oligomers (CN9018 from Sartomer, West Chester, PA). The crosslinker 1,6-hexanediol diacrylate (HDDA from Sigma Aldrich, St. Louis, MO) was used in the 5-12.5 % range. The oligomers were spin coated at 6000 RPM for 60 s to make 35 micron layers. Each layer was cured by exposure to UV light in the absence of oxygen for 120 s. Electrodes were transferred to both sides of each active elastomer layer by stamping single-walled carbon nanotubes (SWCNTs from NanoC, Westwood, MA) from a PTFE filter.

IV. Robot Design

The robot as shown in Figure 3 is 100 mm long, 60 mm high, and 30 mm wide at a mass of 115 g. At this size,

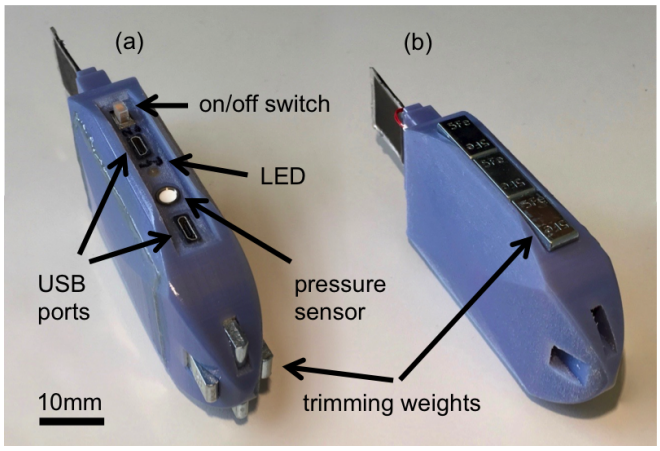

Fig. 3. The reconfigurable robot driven by a soft fin made out of stacked dielectric elastomer actuators. (a) Dorsal side. Diving configuration with all trimming weights placed on the nose. (b) Ventral side. Planar swimming configuration with all trimming weights placed on the belly.

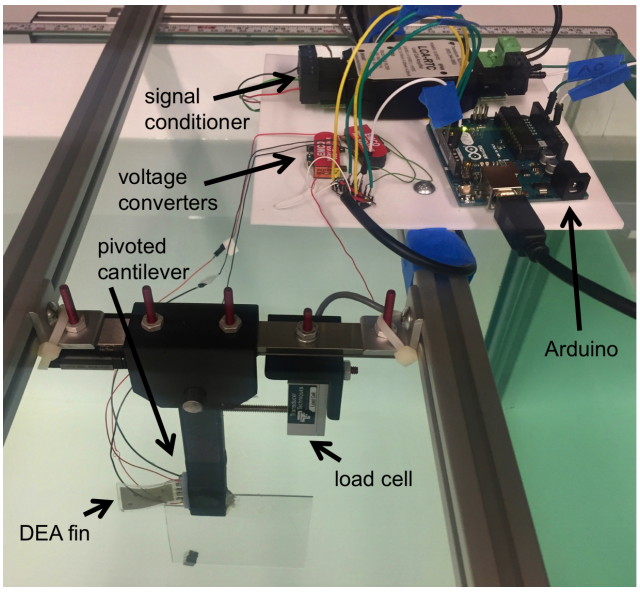

Fig. 4. Our measurement setup installed across the tank. The Arduino commands the voltage converters, which actuate the DEA-fin. The generated thrust force makes the cantilever push on the load cell. The force signal is conditioned by the signal conditioner and read from the Arduino.

its big enough to held all the electronics and small enough to be buoyant. The 3D-printed (Stratasys Objet500) plastic body contains an Arduino Pro Mini microcontroller, an SD card reader/writer for data logging, a Li-Ion battery (7.4 V, 180 mAh), and a power circuit to provide the high actuation voltage to the DEAs. A pressure sensor (TE Connectivity MS5803-02BA) used for depth control, an LED for status indication, two waterproof Micro-B USBs for charging and programming, and an on/off switch penetrate the top end of the body; a ground and two positive supply voltage cables are routed to the DEA driven fin at the back.

The flapping motion of the fin is achieved by alternately switching on and off the two halves of the bimorph DEA (see Figure 2). Any frequency up to 10 Hz can be chosen and controlled by the microcontroller. The amplitude is dependent on the size, strength, and flexibility of the fin and decreases with increasing frequency at a constant applied electric field. The flapping direction is switched at low voltage before one voltage converter (EMCO AG30) per unimorph provides the required actuation voltage of 2 kV.

The robot is slightly positively buoyant and floats at the water surface if not actuated. Its center of gravity (CoG) and swimming direction can be changed respectively by placing external trimming weights. The weight blocks are easily reconnected to either sockets in the nose for vertical diving or to a rail on the belly for planar swimming. They are held in place by magnets mounted internally. The CoG is designed to be below the center of buoyancy in either configuration such that passive stability in pitch and roll is guaranteed.

The total component cost is around USD 300 of which the voltage converters account for 85 %. The assembly of one robot takes about 4 h and includes soldering the circuitry using 36-gauge ultra-flexible wire, mounting the electronic components inside the body with liquid adhesive, water-proofing all penetrating components from the inside with instant epoxy, and finally sealing a lid on the side with plastic bonding epoxy.

V. Experimental Setup

Soft actuators are traditionally less precise than their rigid counterparts, which makes them difficult to quantify. Our experimental setup allowed us to measure the forces generated by the DEA-fins, investigate their consistency, and improve the fin design.

We measured the thrust forces generated by the DEA-fins in a 1.2 m × 0.6 m × 0.5 m glass tank filled with still water. For this purpose, we mounted a rail across the tank, to which we attached a pivoted cantilever and a single-axis load cell (Transducer Techniques GSO-10). The cantilever rigidly connects the submerged fin to the load cell, which is above the waterline. The force generated by the fin causes the cantilever to rotate around a low-friction ceramic ball bearing and push on the load cell. The 100 mN range of the load cell is reached at a compression of 0.1 mm only. Consequently, the maximum angle of rotation in our cantilever design measures 0.2 ° and satisfies a small-angle approximation. We mounted the cantilever and the load cell separately to prevent overloading of the load cell. The signal from the load cell is conditioned (Transducer Techniques LCA-RTC) and measured with an Arduino Uno at 100 Hz. The load cell was calibrated with known loads in air prior to experiments in water. Our values for the static thrust measured in still water are expected to be lower than the dynamic thrust generated during free swimming where vortex shedding adds to the propulsion [26], [27].

Free swimming experiments were performed in the same tank, as well as a larger experimental setup with overhead and side cameras for tracking (described in [28]).

VI. Results

In this section, we present the results from the thrust measurements of the DEAs and the swimming performances

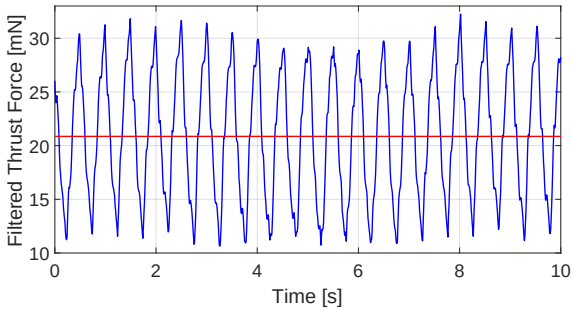

Fig. 5. Time trace of the measured thrust force for a 17 layer fin at 2.0 Hz with its average being shown in red.

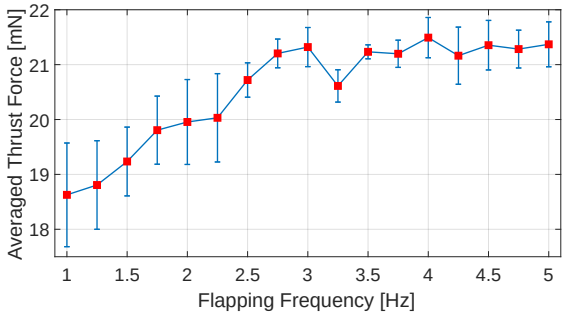

Fig. 6. Average (red squares) and standard deviation (vertical errorbars) of measured thrust forces from five test runs with a 17 layer fin using 10 % HDDA crosslinker.

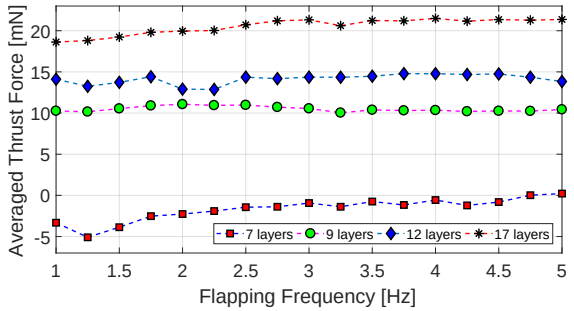

Fig. 7. Dependence of thrust on number of layers in the bimorph (all elastomers contain 10 % HDDA crosslinker).

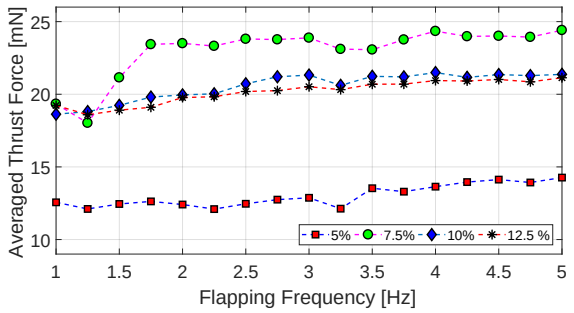

Fig. 8. Dependence of thrust on amount of crosslinker in the elastomer, which dictates material stiffness. All actuators tested were based on 17 layer unimorphs.

of the robot. We kept the size of our DEA-fins constant at 20 mm $\times$ 25 mm and chose a generic rectangular shape to allow for a fair comparison between fins. We varied simple fabrication parameters, such as the number of layers of each fin and the stiffness of the elastomers and measured the force output of the fins. Fluid dynamic considerations were not part of our studies. A model for and information about the thrust production of oscillating fins can be found in [25], [29]. A video of the experiments is included in the supplementary material of this paper.

A. Time trace of the generated thrust force

In a first step, we validated our measurement setup by looking at the time trace of the measured thrust force. The force data in Figure 5 was filtered with an equally weighted and 25 element long moving average filter. The observed sinusoid correlates with our input signal and constitutes the expected thrust pattern as shown in Figure 8 of [25].

B. Thrust forces at various numbers of active layers

In this and the following subsection, we present the resulting thrust forces for a variety of fins actuated at 1.0 Hz to 5.0 Hz in increments of 0.25 Hz. At each frequency, we measured the output thrust force at a sampling rate of 100 Hz for a duration of 10 s and averaged those 1000 samples to a single data point. We repeated this measurement procedure five times per fin and derived the mean and standard deviation as shown for an example 17 layer fin in Figure 6. The five measurements per fin were consistent with each other as the standard deviation was at least an order of magnitude smaller than the measured average force.

Figure 7 shows that the thrust force increases with the number of active layers. There is a threshold thickness under which the fin is too soft and almost no meaningful thrust is generated, as shown by the 7 layer fin. While this result is expected, there is a practical constraint to how many layers can be stacked. Operating these materials at 15-20 V/μm we found each layer to have a 1 % chance of electrical breakdown. For stacks of more than twenty layers the likelihood of breakdown approaches 20 %, which has a significant impact on fabrication yield.

C. Thrust forces at various elastomer stiffnesses

In this experiment, we varied the stiffnesses of the elastomers by tuning the amount of HDDA crosslinker in the starting oligomer precursor from 5 % to 12.5 % corresponding to a Young's modulus of 200 kPa to 500 kPa, respectively. Our earlier model [11], though based on a static configuration, was useful in providing guidelines for the range of material stiffness of interest. The lower limit was set by the minimal stiffness needed to prevent an electromechanical instability, in which the material becomes softer with applied deformation leading to electrical breakdown in the elastomer. The upper limit was set by the Young's modulus of the elastomer: the bimorphs made with elastomers stiffer than 500 kPa did not deform enough to produce measurable thrust at the comparable electric fields. The model predicted the thrust to decrease linearly with increasing stiffness as the

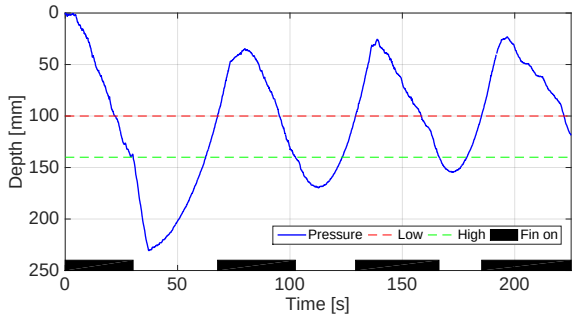

Fig. 9. Closed-loop periodic diving between target depths of 100 mm (low) and 140 mm (high). The solid blue line shows depth as sampled from the pressure sensor at 10 Hz. The black boxes indicate active periods of the fin.

amplitude of each flap decreased at constant field. However, the mass of the water that must be displaced for a successful fin flap reduces the effectiveness of the softer elastomers leading to a peak thrust versus stiffness. Figure 8 shows that the trust force is highest for elastomers containing 7.5 % crosslinker.

D. Maneuvers in planar swimming

The planar swimming experiments were carried out at the water surface. We placed the trimming weights at the robot's belly such that it swims forward in horizontal direction. Straight line swimming was achieved by tuning the symmetry of the oscillation of the fin. The robot can swim circles of various radii when the oscillation is biased towards one side, e.g., by alternately switching on and off only one unimorph. A deliberately biased oscillation can be used to compensate for drift in order to swim exact trajectories.

Based on the results of the thrust measurements we used a 17 layer fin made of elastomer containing 7.5 % crosslinker. Using the lessons from Figure 8 we aimed to operate the robot at the lowest frequency which maximized the thrust output to achieve fast swimming at a lower power. In this case that meant running the fin at 2.2 Hz produced speeds of up to 0.55 BL/s (= 55 mm/s), and turning radii as small as 1.2 BL (= 120 mm), as shown in the supporting video.

E. Vertical diving

Vertical diving enhances the robot's performance from simply swimming on the surface. The robot was reconfigured for swimming in vertical direction by moving the trimming weights to its nose. Altogether, the robot was slightly positively buoyant. The buoyancy made it rise to the surface when the fin was not active. An active fin made it dive in vertical direction at a maximum rate of 0.3 BL/s (= 30 mm/s).

Our robot uses feedback from a pressure sensor to dive controllably. The robot's behavior is updated based on that feedback by a control loop running at 10 Hz. We demonstrated long-range repeatable diving between two thresholds set at 100 mm and 140 mm below an initial depth (Figure 9). The experiment showed significant overshoots caused by the robot's inertia, which could be reduced by applying predictive control strategies.

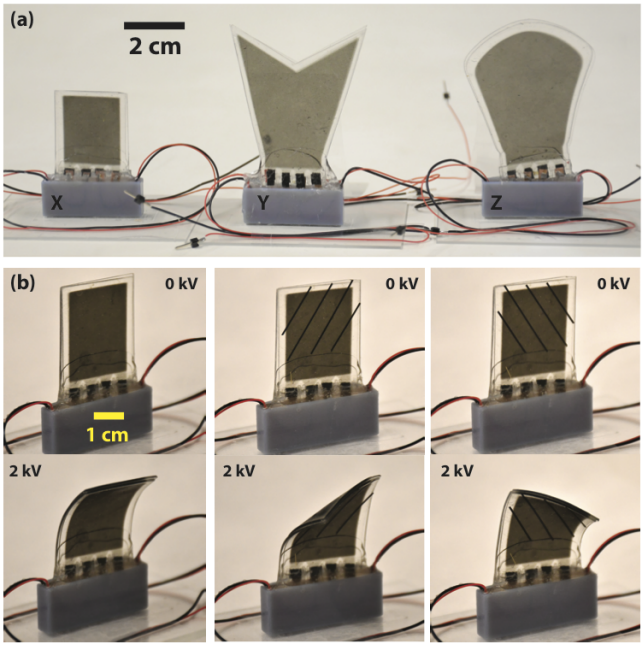

Fig. 10. (a) Different shaped fins - fin X is the geometry used as baseline in thrust experiments. (b) Modification of actuated shape by addition of carbon fiber spars to constrain deformation.

F. Power consumption

The average power consumption is approximately 0.75 W and allows for a robot runtime of more than 100 mins for a 17 layer fin operating at 2.2 Hz. The power consumption increases with the number of active layers per fin as they constitute a higher load.

An approximation of the output power of the robot is defined by its speed times the measured thrust of the mounted fin. The maximum output power was 1.3 mW and results in an overall power efficiency of 0.17 %. We note that neither the robot nor the fin were optimized for efficient swimming.

G. Fin shapes and bending patterns

We kept the fins constant in shape and size for all of the above experiments. However, the final shape of the active part of the fin can be tailored by changing the mask through which the electrode is stamped and the laser-cut pattern to release the fin. Figure 10(a) shows a variety of fin shapes made possible with our manufacturing method, which avoids pre-stretching the DEAs. The thrust measured at low frequency (1 Hz) increased from actuator X (15.5 $\pm$ 0.5 mN), to actuator Y (23.1 $\pm$ 0.4 mN) to actuator Z (26.1 $\pm$ 1.1 mN) consistent with the increasing area. Moreover, the bending path of the DEA can be modified by addition of stiffening spars, as shown in Figure 10(b). Between the custom shape and bending pattern, a wide range of bio-mimetic fins are possible, opening the door for separate studies on efficient fin propulsion.

VII. Conclusions and Future Work

We built active DEA-fins and measured their thrust forces in a standardized setup. Comparative experiments revealed

that the thrust can be increased by stacking additional layers, at the expense of a higher risk of dielectric breakdown. The stiffness of the elastomer can be tuned by modifying the crosslinker concentration to reach peak thrust forces of up to 25 mN.

Our untethered underwater robot achieved a higher degree of autonomy than previous DEA-powered robots by using sensory feedback to update its behavior. The robot demonstrated free planar swimming with speeds of up to 0.55 BL/s (= 55 mm/s) and open-loop turning with radii of 1.2 BL/s (= 120 mm). It can be reconfigured with ease to also demonstrate closed-loop vertical diving at 0.3 BL/s (= 30 mm/s). The swimming performance was enabled by our modular DEA-fin and low footprint power circuitry.

Our results show that by careful selection of components, dielectric elastomer actuators can swim as fast as fluidic-powered actuators. The entire robot occupies a small footprint, comparable to those powered by IPMCs or SMAs, and the actuator fabrication is simple. Our DEAs are scalable in power output, as well as modular, soft, and waterproof. Their modularity allows us to mount multiple actuators on a single robot.

A key limitation of our current robot is the need for two voltage converters per DEA due to low voltage switching. In a next step, we envision a robot with several active fins that is capable of achieving high maneuverability. To this end, we plan to lower the actuation voltages to under 1.2 kV such that switching at high voltage becomes feasible with small enough components and one single voltage converter for several fins will be sufficient. Smaller, simpler, and more maneuverable robots could be implemented in studies of cooperative behavior.

Beyond electrical improvements, the material development space is vast and allows the option to tune the stiffness along the length of our fin. Such tailor made DEAs could be used to study and mimic the undulatory motions of fish fins, for both swimming optimization as well as robotic-inspired biological studies.

References

[1] S. Kim, C. Laschi, and B. Trimmer, "Soft robotics: a bioinspired evolution in robotics," *Trends in Biotechnology*, vol. 31, no. 5, pp. 287–294, 2013.

[2] M. T. Tolley, R. F. Shepherd, B. Mosadegh, K. C. Galloway, M. Wehner, R. J. Wood, and G. M. Whitesides, "A Resilient, Untethered Soft Robot," *Soft Robotics*, vol. 1, no. 00, pp. 1–11, 2014.

[3] M. Wehner, R. L. Truby, D. J. Fitzgerald, B. Mosadegh, G. M. Whitesides, J. A. Lewis, and R. J. Wood, "An integrated design and fabrication strategy for entirely soft, autonomous robots," *Nature*, vol. 536, no. 7617, pp. 451–455, 2016.

[4] C. Majidi, "Soft robotics: a perspectivecurrent trends and prospects for the future," *Soft Robotics*, vol. 1, no. 1, pp. 5–11, 2014.

[5] D. Yang, M. S. Verma, J.-H. So, B. Mosadegh, C. Keplinger, B. Lee, F. Khashai, E. Lossner, Z. Suo, and G. M. Whitesides, "Buckling pneumatic linear actuators inspired by muscle," *Advanced Materials Technologies*, vol. 1, no. 3, 2016.

[6] K. C. Galloway, K. P. Becker, B. Phillips, J. Kirby, S. Licht, D. Tchernov, R. J. Wood, and D. F. Gruber, "Soft robotic grippers for biological sampling on deep reefs," *Soft robotics*, vol. 3, no. 1, pp. 23–33, 2016.

[7] A. D. Marchese, C. D. Onal, and D. Rus, "Autonomous Soft Robotic Fish Capable of Escape Maneuvers Using Fluidic Elastomer Actuators," *Soft Robotics*, vol. 1, no. 1, pp. 75–87, 2014.

[8] M. Rubenstein, A. Cornejo, and R. Nagpal, "Programmable self-assembly in a thousand-robot swarm," *Science*, vol. 345, no. 6198, pp. 795–799, 2014.

[9] Y. Bar-Cohen, *Electroactive polymer (EAP) actuators as artificial muscles: reality, potential, and challenges*. SPIE press, 2004, vol. 136.

[10] R. Pelrine, R. Kornbluh, Q. Pei, and J. Joseph, "High-speed electrically actuated elastomers with strain greater than 100%," *Science*, vol. 287, no. 5454, pp. 836–839, 2000.

[11] M. Duduta, D. R. Clarke, and R. J. Wood, "A high speed soft robot based on dielectric elastomer actuators," in *Robotics and Automation (ICRA), 2017 IEEE International Conference on*. IEEE, 2017, pp. 4346–4351.

[12] M. Duduta, R. J. Wood, and D. R. Clarke, "Multilayer dielectric elastomers for fast, programmable actuation without prestretch," *Advanced Materials*, vol. 28, no. 36, pp. 8058–8063, 2016.

[13] G. Kofod, M. Paajanen, and S. Bauer, "Self-organized minimum-energy structures for dielectric elastomer actuators," *Applied Physics A: Materials Science & Processing*, vol. 85, no. 2, pp. 141–143, 2006.

[14] S. Shian, K. Bertoldi, and D. R. Clarke, "Dielectric elastomer based grippers for soft robotics," *Advanced Materials*, vol. 27, no. 43, pp. 6814–6819, 2015.

[15] R. Pelrine, R. Kornbluh, Q. Pei, S. Stanford, S. Oh, J. Eckerle, R. J. Full, M. A. Rosenthal, and K. Meijer, "Dielectric elastomer artificial muscle actuators: toward biomimetic motion," in *Proc. Spie*, vol. 4695, 2002, pp. 126–137.

[16] J. Eckerle, S. Stanford, J. Marlow, R. Schmidt, S. Oh, T. Low, and S. V. Shastri, "A biologically inspired hexapedal robot using field-effect electroactive elastomer artificial muscles," 2001.

[17] C. Jordi, S. Michel, and E. Fink, "Fish-like propulsion of an airship with planar membrane dielectric elastomer actuators," *Bioinspiration Biomimetics*, 2010.

[18] T. Li, G. Li, Y. Liang, T. Cheng, J. Dai, X. Yang, and B. Liu, "Fast-moving soft electronic fish," *Science Advances*, pp. 1–8, 2017.

[19] J. Shintake, H. Shea, and D. Floreano, "Biomimetic underwater robots based on dielectric elastomer actuators," *IROS*, 2016.

[20] H. Godaba, J. Li, Y. Wang, and J. Zhu, "A soft jellyfish robot driven by a dielectric elastomer actuator," *IEEE Robotics and Automation Letters*, vol. 1, no. 2, pp. 624–631, 2016.

[21] M. Aureli, V. Kopman, and M. Porfiri, "Free-locomotion of underwater vehicles actuated by ionic polymer metal composites," *IEEE/ASME Transactions on Mechatronics*, vol. 15, no. 4, pp. 603–614, 2010.

[22] X. Tan, D. Kim, N. Usher, D. Laboy, J. Jackson, A. Kapetanovic, J. Rapai, B. Sabadus, and X. Zhou, "An autonomous robotic fish for mobile sensing," *Proceedings of the IEEE/RSJ International Conference on Intelligent Robots and Systems (IROS)*, pp. 5424–5429, 2006.

[23] H.-J. Kim, S.-H. Song, and S.-H. Ahn, "A turtle-like swimming robot using a smart soft composite (ssc) structure," *Smart Materials and Structures*, vol. 22, no. 1, 2013.

[24] Z. Wang, G. Hang, J. Li, Y. Wang, and K. Xiao, "A micro-robot fish with embedded SMA wire actuated flexible biomimetic fin," *Sensors and Actuators*, vol. 144, no. 2, pp. 354–360, 2008.

[25] V. Kopman and M. Porfiri, "A miniature and low-cost robotic fish for ethorobotics research and engineering education i: bioinspired design," in *ASME DSCCDynamic Systems and Control Conference*, 2011, pp. pp–MoBT6.

[26] F. Liu, K.-M. Lee, and C.-J. Yang, "Hydrodynamics of an undulating fin for a wave-like locomotion system design," *IEEE/ASME Transactions on Mechatronics*, vol. 17, no. 3, pp. 554–562, 2012.

[27] P. V. y Alvarado and K. Youcef-Toumi, "Design of machines with compliant bodies for biomimetic locomotion in liquid environments," *Journal of dynamic systems, measurement, and control*, vol. 128, no. 1, pp. 3–13, 2006.

[28] F. Berlinger, J. Dusek, M. Gauci, and R. Nagpal, "Robust maneuverability of a miniature low-cost underwater robot using multiple fin actuation," *IEEE Robotics and Automation Letters (RA-L)*, 2017.

[29] R. P. Clark and A. J. Smits, "Thrust production and wake structure of a batoid-inspired oscillating fin," *Journal of Fluid Mechanics*, vol. 562, p. 415429, 2006.